NUMERICAL SIMULATION OF DILUENT EFFECT ON NO_x EMISSION IN A TURBULENT PREMIXED METHANE FLAMES

Subramani A.[1], Ambedkar B.[2], Sarat Chandra Babu[3]
[1]Department of Chemical Engineering, Indian Institute of Technology Madras, Chennai, India
[2]Department of Chemical Engineering, National Institute of Technology Trichy, India
E-mail: [1]subramani@che.iitm.ac.in

ABSTRACT

The stringent requirement to reduce the NO_x from various combustion devices while maintaining the combustor performance is of paramount motivation for the current study. Partially premixing, fuel blends and fuel diluents represents promising approaches for reducing NO_x from flames. A detailed two dimensional, transient numerical study on the later aspect of fuel diluents (helium) to reduce the NO_x emission in a back ward facing step geometry has been carried out using CFX 5.7. The equivalence ratio has been varied from 0.85-1, to study the effect of excess air on NO_x emission. The methane flame is simulated using Eddy break-up model with Zeldovich thermal mechanism for NO_x formation and the turbulence model is w-RSS (Reynolds Shear Stress). The simulation results indicate that considerable reduction in NO_x emission and increase in flame stability can be achieved for a predetermined addition of inert in to the fuel air mixture.

KEYWORDS : Premixed Combustion, Fuel diluent, Flame stability.

I. INTRODUCTION

Numerical simulation has now become a useful research and development tool for the design of combustors. As the scarcity for conventional liquid fuel is ever increasing, gaseous fuels are going to be used extensively. Recently natural gas is being comprehensively used for both stationary combustion systems and vehicular applications. Since natural gas contains mostly methane the present study is intended to investigate two dimensional transient turbulent premixed methane-air-helium flames. There are several research works on methane-air flames using various combustion models. The present work focuses on reduction of NO_x emission by addition of diluents such as helium, because such study has got immense practical relevance.

Barlow and Carter [1] investigated experimentally the effects of temperature and mixture fraction on NO_x emission from H_2 jet flames and focused more on proper measurement of NO_x using laser induced florescence. Hayhurst and Lawrence [2] reported an experimental investigation on NO_x emission in a fluidized bed combustor during burning of coal volatiles and concluded that low rank coal emits more NO_x than high rank coal.

Meunier and Carvalho [3] performed experimental and numerical investigations on the effect of jet Reynolds number on NO_x emission from turbulent propane diffusion flame using laminar flamelet model with thermal and prompt mechanisms for NO_x formation. Schlegel et al [4] reported an experimental-numerical study on NO_x emission from a catalytically stabilized lean premixed methane-air flames. They reported that the NO_x emissions of catalytically stabilized premixed combustion were remarkably lower than those of noncatalytic, premixed combustion.

Many researchers have focused on the development of appropriate NO_x mechanisms for more accurate prediction and investigation of NO_x emission from flames. These include William's mechanism [5], the Leeds mechanism [6], the mechanism discussed by Miller and Bowman [7] and the Zeldovich (1947) thermal mechanism.

The NO_x reduction strategies based on fuel diluents and fuel blends have also been examined. Roberts et al [8] performed an experimental investigation and observed reduction in both NO_x and soot formation using water jet injection. Rorveit et al [9] investigated the effect of diluents such as N_2, CO_2 and He on NO_x formation in H_2-air counter flow flames. They concluded that flames diluted with He and CO_2 produces low NO_x than N_2. Rorveit at al [10] reported an experimental–numerical study on NO_x emission in diluted methane-hydrogen flames.

Many recent studies dealing with NO_x emission have focused on partially premixed flames (PPFs). With regard to their NO_x emission characteristics, Gore and Zhan [11] performed a numerical investigation on the effect of partial premixing on NO_x production in methane–air PPFs and observed the existence of an optimum level of partial premixing that yielded the lowest NO_x emission index. Tanoff et al. [12] conducted a numerical–experimental study of counter flow methane–air PPFs and observed a drastic change in NO_x emission behavior as the flame changed from a merged-

flame to a double-flame structure as the equivalence ratio (φ) was reduced below a certain threshold value. Ravikrishna and Laurendeau [13] also reported a numerical–experimental investigation on the effect of partial premixing on NO_x emission from counter flow methane–air flames. They compared the laser-induced fluorescence measurements of NO_x with predictions using the GRI-2.11 and GRI-3.0 mechanisms and noted that the GRI-3.0 mechanism over predicted NO_x concentrations compared to the measurements and predictions based on the GRI- 2.11 mechanism. A similar observation was made by Barlow et al. [14] in their numerical–experimental study of counter flow methane–air PPFs. Dupont and Williams [15] examined the dominant NO_x formation mechanisms in rich methane–air flames. Sayangdev Nash et al [16] investigated numerically the effect of partial premixing on NO_x emission in a counter flow arrangement using n-heptane and their blends with hydrogen using GRI-3.0 mechanism for flame combined with Li and Williams NO_x mechanism.

The possibility of using fuel blends including fuel diluents to obtain superior pollutant emission characteristics seems to be a promising area of research. While previous investigations have focused on NOx emissions in a variety of flames and configurations, issues pertaining to the use of fuel diluents and fuel blends for reducing NOx emission have not been examined in detail.

Motivated by these considerations the present study is attempted to study numerically the effect of premixing of helium with varying mass fractions and also the effect of equivalence ratio on NO_x emission. All simulations performed in this study are transient and two dimensional.

A. Validation of reaction mechanisms

The mechanism used in the present study is a one step irreversible reaction determined by Wesbrook and Dryer (1981), and is given by;

$$R_{CH4}\ (kgmol/m^3/s) = 2.119 \times 10^{11} \exp[(-2.027 \times 10^8\ J/kgmol)/RT] \times [CH_4]^{0.2} [O_2]^{1.3}$$

Where, concentrations are in units of $kgmol/m^3$. This one step mechanism is very simple and useful tool for describing flame dynamics without complicating the numerical computation. This mechanism was also used by D.G Nortan et al [17] in their numerical study on micro burner. Like wise many researchers have used this mechanism and validated these mechanisms for variety of configurations.

Further the mechanism used for NO_x prediction is Zeldovich which is also commonly used in the literature of combustion. N.Y Sharma et al [18] used Westbrook and Dryer mechanism for methane combustion and Zeldovich thermal mechanism for NO_x prediction, in their study on gas turbine combustor. A.Caldeira-pires et al [19] studied experimentally NO_x formation rates in propane turbulent non premixed jet flames using both thermal (Zeldovich) and Prompt (Fenimore) mechanisms and concluded that Zeldovich mechanism is dominant in lean to stoichiometric laminar premixed flames, and Fenimore mechanism can be dominant under conditions where Zeldovich NO_x is small. Ph. Meunier et al [20] carried experimental and numerical study on formation and destruction NO_x in propane diffusion flames using three different mechanisms for NO_x prediction and concluded that Prompt mechanism in dominant when compared to thermal mechanism. Chen-pang-chou et al [21] studied NO_x formation in laminar Bunsen flames using extended Zeldovich mechanism and validated their predictions. Thus, there exist a substantial validation for the one step kinetics of methane combustion in the literature. However, no attempt is made in the present work to validate it further, instead the reported kinetic parameters have been used as such with out any modifications.

II. SIMULATION DETAILS

Premixed methane-air-helium mixture is fed to the combustor. The geometry used in this work is backward facing step, as shown in Figure-1, which is widely used to validate many turbulence models for the benchmark problems. The dimensions are the one used by Denis et al [22]. The flow field developed in these geometries are complex and exhibits three-dimensional behavior, particularly in the shear layer just behind the step. In order to get proper energy transfer between various turbulent scales developing in these zones, one should perform in principle a full three-dimensional calculations. This kind of computation would require extensive resources. Since the reactive flow with complex chemistry is considered a two dimensional approximation is the choice to limit the computational expense without affecting the accuracy of the predictions.

In the present work ω-RSS (Reynolds shear stress) model is used to account for turbulence and Eddy Break-up model is used for methane flames combined with Zeldovich thermal and prompt mechanisms for NO_x formation. It is worth noting that transient RANS (TRANS) can be used in place of LES (large eddy simulation) as it requires less computational time with reasonably good prediction of turbulent structures. In the present study the effect of radiation is neglected (just to reduce the time of computation) and it can be justified by fact that turbulent

flames have less residence time inside the chamber for radiation to be predominant and even if included the decrease in temperature would be only 10-20 K (Rorveit et al, [10]) and the resultant variation in NO_x prediction may not vary much.

III. FLAME MODELING

A. Eddy break-up model

The Eddy break-up Model [23] is based on the concept that the chemical reaction is fast relative to the transport processes in the flow. The model assumes that the reaction rate may be related directly to the time required to mix reactants at the molecular level. In turbulent flows, this mixing time is dominated by the eddy properties, and therefore, the rate is proportional to a mixing time defined by the turbulent kinetic energy k and eddy dissipation ε. This concept of reaction control is applicable if reaction rates are fast compared to reactant mixing rates. In CFX 5.7, Eddy break-up model is combined with a Chemical Timescale to simulate local extinction, with an Extinction Temperature to disable the reaction wherever the temperature is less than the specified extinction temperature, and with a Mixing Rate Limit to define the maximum allowed value of the local turbulent mixing rate. This model sometimes predicts unphysical behavior, e.g. the flame creeping across walls [24]. This is because the ratio of the turbulence quantities ε/k becomes large close to wall boundaries, but the turbulence in these regions is low. The mixing rate limit is used to enforce an upper limit on the value ε/κ used for computing the reaction rate.

B. Governing Equations

The governing equations of the present problem have been listed out below.

Continuity;

$$\frac{\partial \rho}{\partial t} = -\rho \frac{\partial U_i}{\partial x} \tag{1}$$

ω-RSS model;

Averaged momentum equation;

$$\frac{\partial}{\partial t}\left(\rho\overline{u_i u_j}\right) + \frac{\partial}{\partial x}\left(U_k \rho \overline{u_i u_j}\right) = P + \phi_{ij} + \frac{\partial}{\partial x}\left[\left(\mu + \frac{2}{3} c_s \rho \frac{\kappa^2}{\varepsilon}\right)\frac{\partial \overline{u_i u_j}}{\partial x}\right] - \frac{2}{3}\delta_{ij}\rho\varepsilon$$

$$P = -\rho\left(\overline{u \otimes u}(\nabla U)^T + (\nabla U)\overline{u \otimes u}\right) \tag{2}$$

$$\phi_{ij} = \phi_{ij1} + \phi_{ij2} \tag{3}$$

$$\phi_{ij1} = -\rho\varepsilon\left(C_{s1} a + C_{s2}\left(aa - \frac{1}{3} a.a\delta\right)\right) \tag{4}$$

$$\phi_{ij2} = -C_{r1} Pa + C_{r2}\rho\kappa S - C_{r3}\rho\kappa S\sqrt{a.a} + C_{r4}\rho\kappa\left(aS^T + Sa^T - \frac{2}{3} a.S\delta\right) + C_{r5}\rho\kappa\left(aW^T + Wa^T\right) \tag{5}$$

$$a = \frac{\overline{u \otimes u}}{\kappa} - \frac{2}{3}\delta \tag{6}$$

$$S = \frac{1}{2}\left(\nabla U + (\nabla U)^T\right) \tag{7}$$

$$W = \frac{1}{2}\left(\nabla U - (\nabla U)^T\right) \tag{8}$$

ω-equation;

$$\frac{\partial(\rho\omega)}{\partial t} + \frac{\partial}{\partial x}\left(\rho U_k \omega\right) = \alpha\rho\frac{\omega}{k} P_k - \beta\rho\omega^2 + \frac{\partial}{\partial x}\left[\left(\mu + \frac{\mu_t}{\sigma}\right)\frac{\partial\omega}{\partial x}\right] \tag{9}$$

σ = 2 ;
β = 0.075;
α=5/9;
C_{r1} = 0.0;
C_{r2} = 0.8;
C_{r3} = 0.0;
C_{r4} = 0.6;
C_{r5}=0.6;

Energy ;

$$\frac{\partial}{\partial t}(\rho h) = -\left[\frac{\partial}{\partial x}(\rho h U_i) + \frac{\partial}{\partial x}\left(\rho h U_j\right)\right] + \frac{\partial\left(k_f \frac{\partial T}{\partial x}\right)}{\partial x} + \frac{\partial\left(k_f \frac{\partial T}{\partial y}\right)}{\partial y} + \sum_i \left[\frac{\partial\left(h_i \rho D_i \frac{\partial Y_i}{\partial x}\right)}{\partial x} + \frac{\partial\left(h_i \rho D_i \frac{\partial Y_i}{\partial x}\right)}{\partial x}\right] - \sum_i h_i R_i \tag{10}$$

Species ;

$$\frac{\partial}{\partial t}(\rho Y_i) = -\left[\frac{\partial(\rho Y_i U_i)}{\partial x} + \frac{\partial\left(\rho Y_i U_j\right)}{\partial y}\right] + \frac{\partial\left(\rho D_i \frac{\partial Y_i}{\partial x}\right)}{\partial x} + \frac{\partial\left(\rho D_i \frac{\partial Y_i}{\partial y}\right)}{\partial y} + R_i \tag{11}$$

Ri $\propto \frac{\varepsilon}{\kappa}$ (Eddy break-up model) with A=4; B=0.5 (model constants)

The details of the initial conditions are given in table-1 and table-2.

Table-1. Inlet Conditions

Case	φ	T inlet (K)	P(Kpa)
1	1	300	101
2	0.85	300	101

Table-2. Feed Composition

Case	% He*	CH_4 mass fraction	O_2 mass fraction	Mass flow rate (kg/s)
1	0	0.055	0.2193	1.0531e-04
	5	0.0529	0.2116	1.0911e-04
	10	0.05187	0.2075	1.1130e-04
	15	0.0494	0.1978	1.1671e-04
2	0	0.047	0.2180	1.2285e-04
	5	0.0453	0.2103	1.2736e-04
	10	0.0438	0.2030	1.3188e-04
	15	0.04233	0.19633	1.3640e-04

*mass percent (percentage of incoming nitrogen)

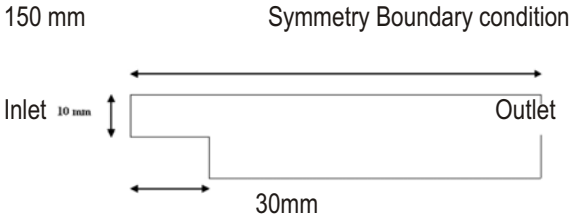

Fig .1 Schematic of computational domain along with a description of some boundary conditions.

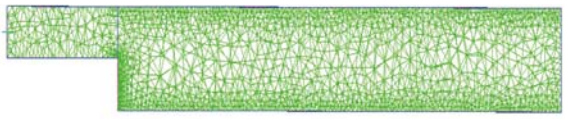

Fig .2 Unstructured mesh used in this model generated using ICEM CFD

IV. SOLUTION METHODOLOGY

CFX 5.7 (ANSYS) uses a coupled solver, which solves the hydrodynamic equations (for *u*, *v*, *w*, *p*) as a single system on a co-located mesh. And for transient analysis it uses first order backward Euler scheme with high resolution differencing scheme. In the present simulation a non-uniform mesh is used with more nodes accumulated near the reaction zone as shown in Fig .2 Since combustion is highly transient phenomena, in this work transient simulations are carried out which will give more insight to the problem than steady state simulations even though it consumes more time. To be more specific transient simulations are carried out for the total time of 0.0255 s using a time step of 2.55μs. Computations are initially carried out on coarse grid and later on a fine grid. It is found that very fine mesh offers no good advantage other than consuming more time. The results are shown in Fig .3 in which temperature was plotted against axial distance for different mesh densities. All the work presented in this work is achieved using mesh consisting of 4997 nodes.

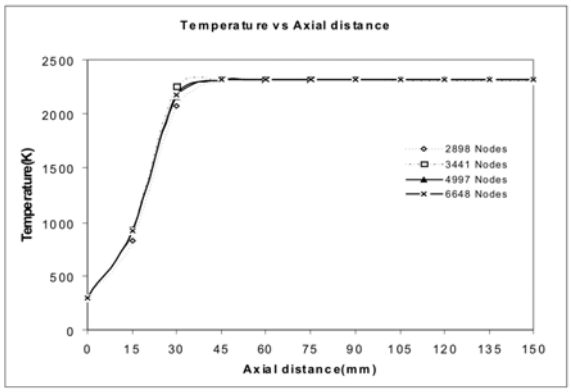

Fig .3 Temperature profile along the axial distance of methane-air flame of φ=1 with different mesh densities.

V. RESULTS AND DISCUSSION

A. Combustion characteristics

The reactive simulations presented in this section are carried in the geometry (Figure-1) with symmetry condition imposed on the side walls in X-direction. In principle one should not impose symmetry on the large scale eddies but it has been observed that symmetry modes are favored in reactive flows (Denis Thaibaut [22]). The inlet air-fuel mixture temperature is 300 K and the geometry wall boundaries are adiabatic.

For all the cases studied combustion characteristics such as reaction rate, species mass fraction, flame speed, flame shape and temperature are summarized in this section. Figure-4a&4b shows the concentration profile of methane for φ = 1 and 0.85 for various helium proportion along the centerline. Combustion efficiency remains unchanged due to premixing of helium with the inlet air fuel mixture as observed from the Fig .4a & 4b. As helium is an inert gas and does not participate in combustion reaction, its presence is only to reduce the combustion temperature. The reduction of flame temperature by the addition of helium is found to be linear for both case-I and II as shown in Fig .4c.

Fig .5 depicts the reaction rate and temperature along the centerline of the burner for case-I with zero percent helium. Three regions can be identified namely preheating, combustion, and post-combustion (D.G. Norton [17]). In the preheating region , once the fluid reaches the ignition temperature of approximately 1000° C (region I) , the mixture combusts rapidly , releasing heat which causes sharp rise in the fluid temperature in region II and the fluid reaches adiabatic flame temperature in this zone. In the post–combustion (region III), after the reactants have been consumed, the reaction stops, as indicated by steep fall in the rate of reaction of methane. Similar profiles are observed for different fractions of helium.

Fig .6(a-d) shows the concentration profiles of N_2, H_2O, CO2 and O_2 plotted against axial distance for different fractions of helium for case-I i.e., stoichiometric ratios of fuel-air mixture. The concentration of products increases slowly from region II and attains a constant value as the flame stabilizes in region III. These profiles confirm that addition of helium do not affect the combustion rate. Similar profiles are observed with excess oxygen (not shown). The effect excess oxygen on NO_x production is explained in the next section.

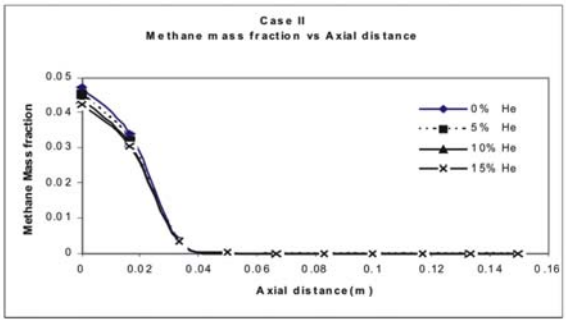

Fig .4a Methane mass fraction along axial distance for case-I

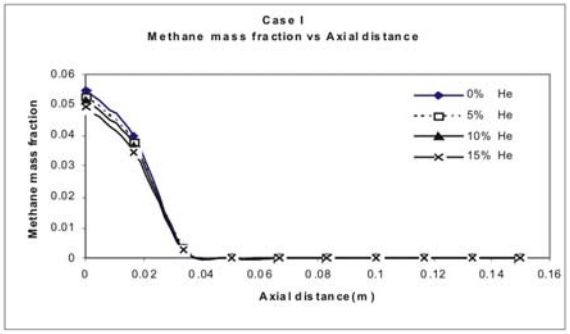

Fig .4b Methane mass fraction along axial distance for case-II

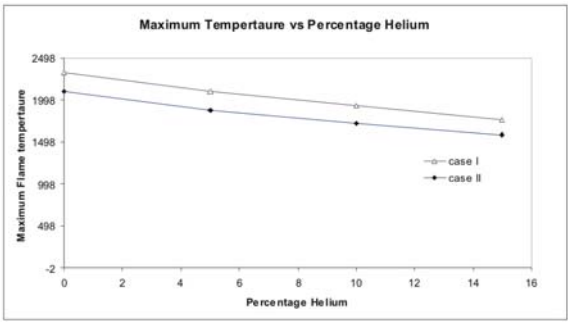

Fig .4c Variation of maximum flame temperature with respect mass fraction of Helium.

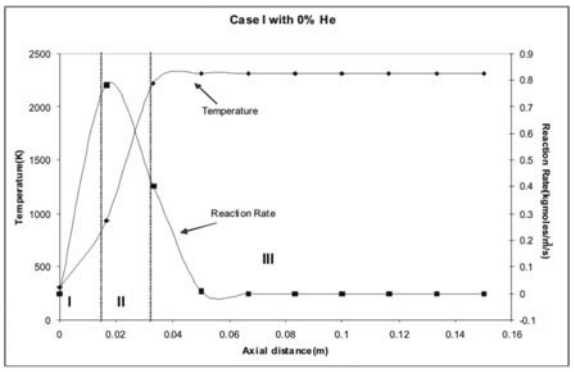

Fig .5 Temperature and reaction profiles along the centerline. Three regions are shown here: I. Preheating, II. Combustion, III. Post-combustion.

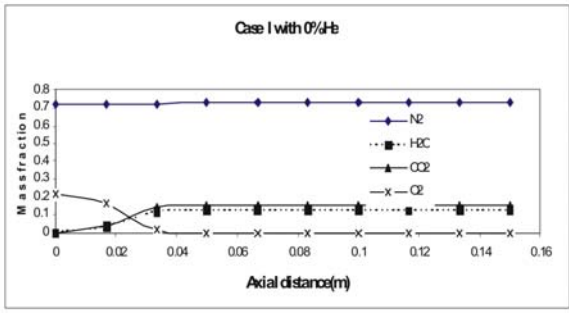

(6a)

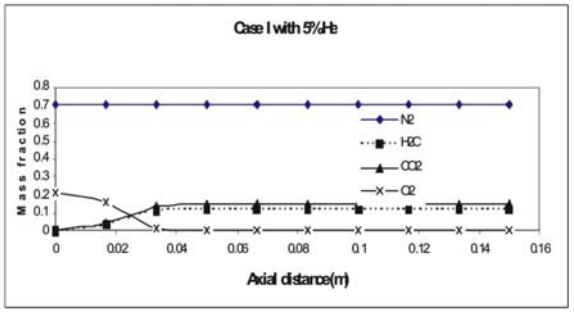

(6b)

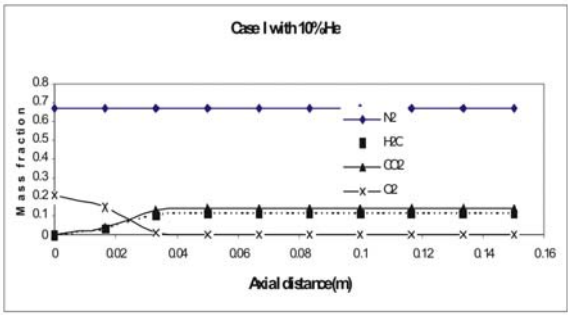

(6c)

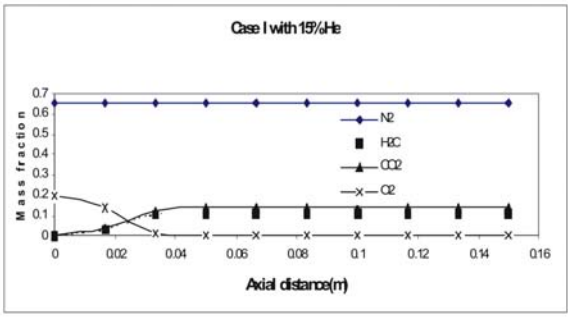

(6d)

Fig .6 (a-d) concentration profiles of N_2, H2O, CO2 and O_2 along the axial direction for φ=1.

B. Effect of Helium and excess air on NO_x emission

Owing to the lower flame temperature with the addition of helium, it might be expected to give positive impact on NO_x emissions. In the present simulations it is observed that there is a drastic reduction in NO_x mass production rate as the helium addition is increased. However, it is noted that the concentration levels of the NO_x, in both pure and diluent added methane flames, is found to be more near the recirculation regions i.e. behind the step where the flue gas has more residence time. The residence time of the reaction products in the high-temperature reaction zone is the main physical effect associated with NO_x formation [3].

In Fig .7 (a-d) NO_x mass fraction contours are shown for Ø = 1 in the middle plane at z = 0.5 mm. It is observed that the NO_x level is high just behind the step as expected. Similar contours are obtained for other cases also (not shown).

Fig .8 (a-d) compares the rate of formation of NO_x by both thermal and prompt mechanisms for case-I. It is found that for all the cases thermal mechanism dominates prompt mechanism. Most of the NO_x production takes place only in the post combustion region where the flame stabilizes with adiabatic flame temperature of about 2300 K in which 90% of the NO_x formed will be through thermal mechanism. This is in good agreement with the literature that for premixed combustion when the flame temperature is above 1800 K thermal mechanism will be predominant over prompt mechanism. The global NO_x characteristics of pure methane and diluent added methane flames can be better compared by plotting emission index as a function diluent percentage for case-1 and case-2 as shown in Fig .9. The emission index is defined as

$$EINO_x = \frac{1000\int_0^L M_{NOx}\omega_{NOx}\,dx}{-\int_0^L M_{CH4}\omega_{CH4}\,dx} \quad \text{(g/kg of fuel)}$$

Here M represents the molecular weight ω& is the net production or consumption rate, L is the distance between the inlet and outlet and x is the axial coordinate. The emission index is a global parameter that has been commonly used to characterize NO_x emission from different flames (Sayangdev Naha [16]). Figure-ure-9 depicts that when no helium is mixed, the $EINO_x$ is higher for φ<1 than φ=1, it is because of the formation more [O] radicals as given by the following expression

$$\frac{1}{2}O_2 \Leftrightarrow O \quad \text{(Westenberg, 1975)}$$

$$[O] = 12567[kmol^{1/2}m^{-3/2}K^{1/2}].T^{1/2}\exp(-31096/RT)[O]^{1/2}$$

However the premixing of helium overcomes this problem for φ=0.85 just by taking large amount of heat of reaction as it has high thermal conductivity (Geir j. Rørtveit [10]) as indicated by an intersection point in the Figure-.9 (shown by an arrow).

C. Flame stability

Here the turbulent flame speed is taken as the measure of flame stability (Evatt R.Hawkes et al [25]). A higher turbulent flame speed may allow the enriched flame to better resist flame blow-off. In the present study turbulent flame speed closure developed by Zimont et al [26] is used. i.e.

$S_t = AGu'^{3/4}s_L^{1/2}\lambda_u^{-1/4}l_t^{1/4}$

Where A=0.5 (modeling coefficient)

G stretching factor accounts for reduction of the flame velocity due to large strain rate

s_L laminar burning velocity

λ_u thermal conductivity of unburnt mixture

$u' = \sqrt{\frac{2}{3}\kappa}$ turbulent velocity fluctuations

$l_t = \kappa^{2/3}/\varepsilon$ integral turbulent length scale.

In Fig .10 flame speed is plotted against axial distance for the case-with φ=1 and for different fractions of helium. Similar profiles are obtained for other cases also (not shown). It is readily observed that the turbulent flame speed for helium mixed methane flame is slightly higher than that of pure methane flame. The increase in mass flow rate of the helium mixed methane flame enhances the overall heat transfer coefficient, turbulent effects, and flame area. It is observed in region II the flame speed is steeper than that in the region I. In region III the flame speed decreases slowly as flame approaches the outlet; it is because of the stretching effects of the flame.

But to emphasize more on flame stability, flame stretch effects, thermal diffusive effects and flame annihilation are to be studied in detail. In addition to that wall effects on stability which is not considered in the present work should also be considered (J.Andrae, [27]).

(7a) 0% Helium

(7b) 5% Helium

(7c) 10% Helium

(7d) 15% Helium

Fig .7(a-d) Contours of NO_x distribution in the middle plane at z=0.5mm for φ=1

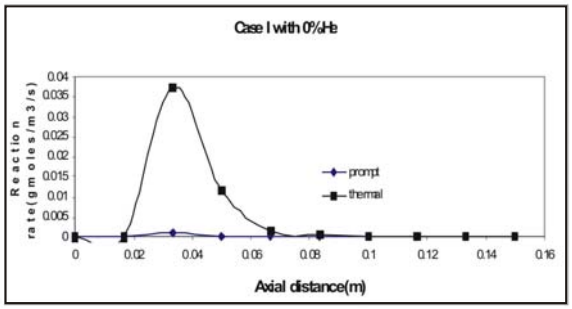

(8a)

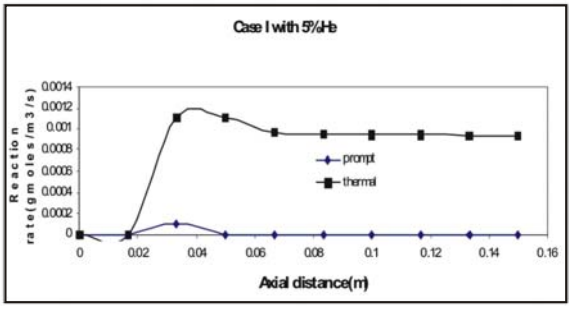

(8b)

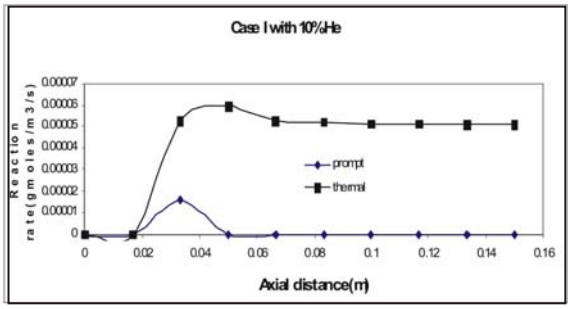

(8c)

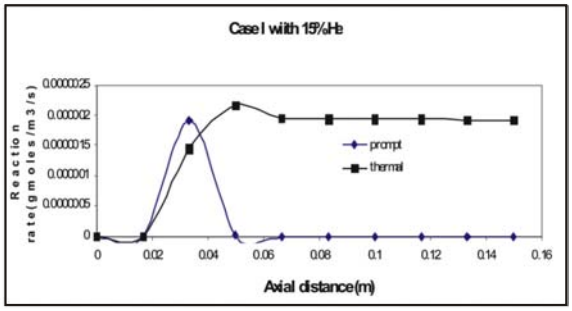

(8d)

Fig .8(a-d) Reaction rates of thermal and prompt mechanisms for φ=1 case-along axial distance.

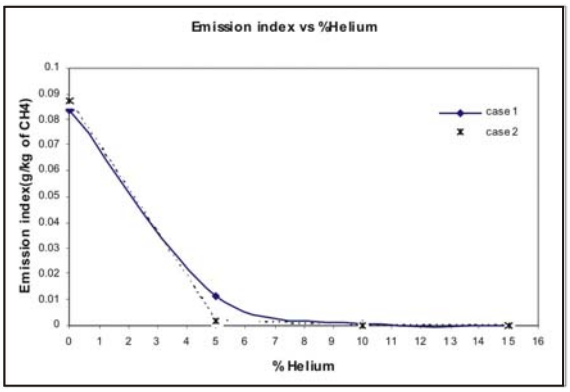

Fig .9 Emission index as a function percentage helium mixed for case-I and II.

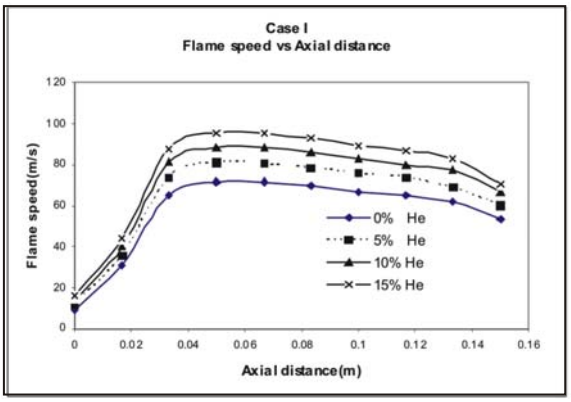

Fig .10 Flame speed along the axial distance for φ=1.

VI. CONCLUSION

In this work numerical simulations have been carried out to study the effect of diluent helium on NO_x emission in two-dimensional backward facing step geometry. The effect helium on NO_x emission has been investigated for two cases by varying the equivalence ratio 0.85-1. The analysis of the result indicates that premixing of helium with air-fuel mixture considerably reduces the adiabatic flame temperature and thus reducing the rate of formation NO_x without affecting the conversion efficiency of the fuel. The increase in turbulent flame speed is observed for helium mixed flames. These simulations have been carried out using TRANS (transient RANS simulation) instead of LES which is widely used in combustion studies. Simulation results indicate that TRANS can be used for predicting the Nox formation.

Nomenclature

a	anisotropy tensor
C_s	Reynolds stress model constant (0.22)
D	diffusion coefficient
h	enthalpy
k_f	thermal conductivity
P	shear production term
R	reaction rate
S	strain rate
T	temperature
t	time
U	average velocity
u	instantaneous velocity
W	vorticity
Y	species
x, y, z	coordinates
ε	eddy dissipation
κ	turbulence kinetic energy
ρ	density
ω	turbulence frequency $\frac{([fuel]/[air])_{actual}}{([fuel]/[air])_{stoich}}$

Subscript

i	i^{th} species, x-direction
j	y-direction
k	z-direction
t	turbulent property

REFERENCES

[1] R.S. Barlow, C.D. Carter, Relationship among nitric oxide, temperature and mixed fraction in hydrogen jet flames, Combustion and Flame 104 (1996) 288–299.

[2] A.N. Hayhurst, A.D. Lawrence, The Amounts of NO, and N_2O formed in a Fluidized bed combustor during the burning of coal volatiles and also of char, Combustion and Flame 105 (1996) 341–357.

[3] M.C. Meunier, M.G. Carvalho, On NO_x emissions from turbulent propane diffusion flames, Combustion and Flame 112 (1998) 221–230.

[4] A. Schlegel, P. Benz, T. Griffin, W. Weisenstein, H. Bockhorn, Catalytic stabilization of lean premixed combustion method for improving NO_x, emissions, Combustion and Flame 105 (1996) 332–340.

[5] S.C. Li, F.A. Williams, NO_x formation in two-stage methane-air flames, Combustion and Flame 118 (1999) 399–414.

[6] Leeds NOx mechanism, http://www.chem.leeds.ac.uk/combustion/nox.html.

[7] J.A. Miller, C.T. Bowman, Progress, Energy Combustion Science, 15 (1989) 287.

[8] C.E. Roberts, Determination of the effect of water on soot formation, http://www.swri.edu/3pubs/IRD1999/03907399.htm .

[9] G.J. Rortveit, J.E.Hustad, S.C. Li, F.A.Williams, Effects of diluents on NO_x formation in hydrogen counter flow flames, Combustion and Flame 130 (2002) 48–61.

[10] G.J. Rortveit, J.E. Hustad, F.A. Williams, 'NO_x formation in diluted CH_4/H_2 counter flow diffusion flames', proceedings of 6th international conference on technologies and combustion for clean environment, Porto, Portugal.

[11] J.P. Gore, N.J. Zhan, NO_x, emission and major species concentrations in partially premixed laminar methane/air co-flow jet flames, Combustion and Flame 105 (1996) 414–427.

[12] M.A. Tanoff, M.D. Smooke, R.J. Osborne, T.M. Brown, R.W. Pitz, Proc. Combustion Institution, 26 (1996) 1121–1128.

[13] R.V. Ravikrishna, N.M. Laurendeau, Laser-induced fluorescence measurements and modeling of nitric oxide in counter flow partially premixed flames, Combustion and Flame,122 (2000) 471–482.

[14] R.S. Barlow, A.N. Karpetis, J.H. Frank, J.Y. Chen, Scalar profiles and no formation in laminar opposed-flow partially premixed methane/air flames, Combustion and Flame 127 (2001) 2102–2118.

[15] V. Dupont, A. Williams, NO_x mechanism in rich methane-air flames, Combustion and Flame 114 (1998) 103–118.

[16] Sayangdev Naha, Suresh K. Aggarwal, Fuel effects on NO_x emissions in partially premixed flames, Combustion and Flame, 139 (2004) 90–105.

[17] D.G.Nortan, D.G.Vlachos, Combustion characteristics and flame stability at the micro scale: a CFD study of premixed methane/air mixtures, Chemical Engineering Science 58, (2003), 4871-4882.

[18] N.Y. Sharma, S.K. Som, Influence of fuel volatility and spray parameters on combustion characteristics and NO_x emission in a gas turbine combustor, Applied Thermal Engineering 24, (2004) 885–903.

[19] A.Caldeira-Pires, and M.V.Heitor, Characteristics of nitric oxide formation rates in turbulent nonpremixed jet flames, Combustion and Flame 120,383–39 (2000).

[20] Ph. Meunier, M. Costa and M. G. Carvalho, The formation and destruction of NO_x in turbulent propane diffusion flames, Fuel Vol. 77, No. 15, pp. 1705–1714, 1998.

[21] Chen-Pang Chou, Jyh-Yuan Chen, Clement G. Yam, and Kenneth D. Marx, Numerical modeling of NO_x formation in laminar bunsen flames—a flamelet approach, Combustion and Flame 114:420–435 (1998).

[22] Denis Thibaut and Sebastian Candel, Numerical study of unsteady turbulent premixed combustion: application to flashback simulation, Combustion and Flame 113:53-65, 1998.

[23] Magnussen BF, Hjertager BH. “On mathematical models of turbulent combustion with special emphasis on soot formation and combustion”, 16th symposium on combustion Cambridge, MA 1976 p.719-729.

[24] N. N.: ANSYS CFX-5, Version 5.7, User Help - Combustion modeling.

[25] Evatt R. Hawkes, Jacqueline H. Chen, Direct numerical simulation of hydrogen-enriched lean premixed methane-air flames, Combustion and Flame 138 (2004) 242–258.

[26] Zimont.V.L, Polifke.W, Bettelini.M and Weisenstein.W. “An efficient Computational Model for Premixed Turbulent Combustion at High Reynolds Numbers based on a Turbulent Flame Speed Closure”.J. Engineering for Gas Turbines and Power (Transactions of the ASME), vol 120, pp. 526-532, 1998.

[27] J.Andrae and P.Bjornbom and L.Edsberg, Numerical study on wall effects with laminar methane flames, Combustion and Flame 128:165-180(2002).

Mr. Subramani Adhi is a Research scholar in Indian Institute of Technology, Madras . He has been working on liquid sodium pool combustion and on developing a comprehensive combustion model for modeling liquid metal pool combustion. He was recipient of the innovative student project award of Rs.2 lakhs for the project on vapor jet combustion of liquid sodium in co-flow configuration from IIT Madras. He has developed a pool spreading model for an accidental spill of liquid sodium under pool fire conditions.